Calibration of in situ magnetic susceptibility measurements

J. Gattacceca, Philippe Eisenlohr, Pierre Rochette

Geophys. J. Int. (2004) **158,** 42–49 doi: 10.1111/j.1365-246X.2004.02297.x

Calibration of *in situ* magnetic susceptibility measurements

Jérôme Gattacceca, Philippe Eisenlohr and Pierre Rochette

CEREGE, CNRS-Université Aix Marseille 3, BP 80, 13545 *Aix-en-Provence Cedex* 4, *France. E-mails: gattacceca@cerege.fr (JG); rochette@cerege.fr (PR)*

Accepted 2004 March 25. Received 2004 March 12; in original form 2003 October 10

SUMMARY

The aim of this work is to calibrate a magnetic susceptibility field probe (SM30) in order to allow measurement on natural boulders of any shape and size. This calibration was performed through measurements on pebbles of different shapes, sizes and lithologies. We model a correction factor (geometric factor) that has to be applied to the SM30 measurement to obtain the real volume magnetic susceptibility of a sample of known volume. This geometric factor depends mostly on the volume of the sample, and to a lesser extent on its shape. We also present an original magnetic measurement scheme that provides, with three SM30 measurements at different distances, an estimation of the volume of a sample. By combining the two calibration models, it is possible to obtain the volume magnetic susceptibility of a natural sample with only three SM30 measurements, without requiring additional information such as sample volume. On the other hand, the calibration performed on a semi-infinite homogeneous body with variable measuring distance leads to a 2-D model of the SM30 response over its integration volume and allows the determination, with a sufficient number of discrete measurement at variable distance, of the thickness and susceptibility of the different layers of a composite body. Both types of calibration were successfully validated on natural or synthetic samples. Therefore the SM30 portable susceptometer appears to be a suitable instrument to perform *in situ* magnetic susceptibility measurement of individual boulders or to establish magnetic susceptibility profiles. In addition, the modest dimensions of the probe and the relative simplicity of the proposed measurement schemes should enable automation of the measurements that could find applications for robotic exploration of solid bodies of the solar system, for example.

Key words: calibration, contact probe, magnetic susceptibility, susceptibility profile, volume measurement.

1 INTRODUCTION

Volume magnetic susceptibility K is a dimensionless parameter defined as the derivative of the intensity of the magnetization induced in a sample ($M = mV$, m being the magnetic moment and V the sample volume) with respect to the applied magnetic field. This intrinsic property can be routinely measured in the laboratory with susceptometers, acknowledging the fact that it requires a separate volume measurement. Magnetic susceptibility measurements have numerous fields of application as they provide information about the concentration and nature of iron phases. Weathering profiles (Mathé *et al.* 1999), pollution monitoring (Heller *et al.* 1998), classification of granitoids (Ishihara 1977), correlation between sedimentary cores and palaeoclimatic proxy (Thouveny *et al.* 1994), ash-layer detection in deep-sea sediments core (Touchard & Rochette 2004), meteorite classification (Rochette *et al.* 2003) and aid in interpretation of magnetic anomalies are a few applications.

In this paper, we present and calibrate a magnetic susceptibility measurement scheme that does not necessitate independent volume measurements and can be easily used *in situ* and automated. We show that this measurement scheme allows the determination of the volume magnetic susceptibility of finite samples in their natural shape and volume, and of susceptibility profiles of a soil, for example.

2 MATERIAL AND METHODS

From the various existing susceptibility field probes we selected the SM30 probe supplied by ZH instruments. It contains an *LC* circuit with a 6 cm diameter, 1 cm thick copper coil that creates a small alternating field (50 μT at probe contact, 8 kHz). The resonance frequency of this oscillating *LC* circuit is modified when a sample is placed close to the sensor. The variation in resonance frequency between a blank measurement and sample measurement is translated into volume magnetic susceptibility expressed in SI. A second blank measurement allows the evaluation and correction of the instrumental drift. Sensitivity is 10^{-7} SI and maximum measurable susceptibility is 1 SI for the upgrade version (0.1 SI for the standard version). The acquisition time is a few seconds.

Magnetic susceptibility is measured over a volume that we call the integration volume. The value given by the SM30 corresponds to the actual volume magnetic susceptibility only if the measured

sample fills the whole integration volume. If the sample is smaller than the integration volume, the measured volume susceptibility appears lower than its real value. If the sample is larger, only the part contained in the integration volume will contribute to the measurement. In this latter case, the measured susceptibility will be the real one if the sample is homogeneous.

In order to calibrate the SM30 measurements for small objects and to model its response to heterogeneous samples we used a Kappabridge KLY2 Geofysika susceptometer as a reference. This apparatus measures susceptibility in a low alternating field (400 μT, 920 Hz) and provides precise measurements with a resolution of 5×10^{-8} SI. It has been cross-calibrated in different laboratories to within 1 per cent (Sagnotti *et al.* 2003). We used both standard and large pick-up coils, with an inner diameter of respectively 4 and 8 cm.

3 CALIBRATION

The first step of calibration is to evaluate the response of the SM30 for homogeneous discrete objects of different shapes, sizes and volume susceptibility. For this purpose, 315 volcanic pebbles of different lithology (60 of phonolite and agpaite, 143 of aphyric basalts and 112 of porphyric basalts) were collected in the riverbed of the Eysse (Ardèche, France). Due to an active transport of less than 10 km (average slope 4 per cent) their shape is rather irregular. An additional 56 marly limestone pebbles of nearly perfect ellipsoidal shapes were collected in the large Alpine Durance river (Bouches du Rhône, France). Pebble masses ranged from 0.85 to 755 g. Their shape is approximated by an ellipsoid whose three principal dimensions were measured with a calliper. Care was taken during sampling to retrieve only homogeneous samples but to regularly cover the shape and size spectra.

Pebble homogeneity was tested on four samples by drilling a core (2.5 cm in diameter) into them, cutting it into 2 mm slices and measuring the magnetic susceptibility of each slice (Fig. 1). The pebbles appear to be homogeneous with variations of ± 10 per cent around the mean value. In particular, no strong difference is observed between the subsurface and the core of the pebbles. They can thus be considered as magnetically homogeneous bodies and are suitable for calibration. In order to complete the calibration for larger objects which would not fit in the large KLY2 coil we used 'synthetic pebbles' hand-made from pottery clay. The calibration was performed by measuring the volume susceptibility of these objects with both the SM30 and the KLY2. The two apparatuses operate

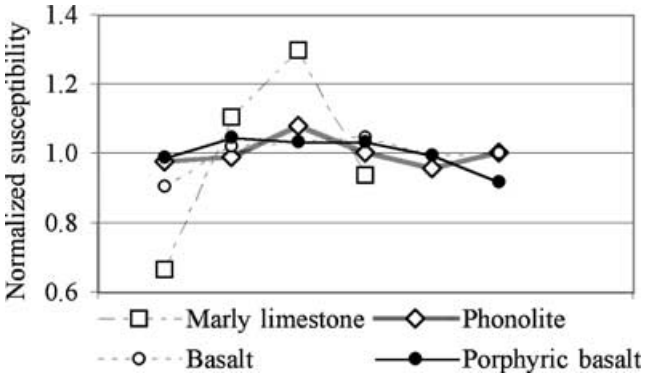

Figure 1. Magnetic susceptibility of successive slices of a core normalized to mean susceptibility of the core for four different pebbles. The core length is 2 to 3 cm.

at different frequencies and magnetic fields, but the magnetic susceptibility is neither frequency- nor field-dependent for the rather large magnetite grains contained in our samples. Moreover, even in unfavourable cases (presence of superparamagnetic magnetite, haematite, pyrrhotite), the variability of susceptibility with field intensity and frequency is only a few per cent at most, well within the expected accuracy of the calibration.

To determine the volume susceptibility of the pebbles with the KLY2 it is necessary to evaluate their volume. For this purpose, the mean density for each lithology was evaluated following an Archimedean method developed by Consolmagno & Britt (1998) using 40 μm glass spheres as a fluid and 20 large glass spheres of various diameters to calibrate the method. The density of clay ($(2.07 \pm 0.03) \times 10^3$ kg m^{-3}) was determined by weighing 10 samples of known volume. An additional parameter to determine is the anisotropy of magnetic susceptibility. Indeed, rocks are generally anisotropic and this effect has to be evaluated as it represents a limit to the reproducibility of susceptibility measurements along a single direction and therefore a limit to the accuracy of a comparison between two susceptibility measurements with different instruments. Anisotropy of magnetic susceptibility was evaluated for 34 samples following standard procedures with measurements along 15 directions. Degrees of anisotropy, defined as the ratio between maximum and minimum susceptibilities, are low (<1.1) for all lithologies and especially for the two types of basalts (<1.04). Therefore the volume magnetic susceptibility of the pebbles was measured along a single arbitrary direction with the KLY2. Knowing the mass and density of each pebble, we obtained the reference volume susceptibility values, denoted by K_r (Table 1). Values range from -1×10^{-6} (marly limestone sample) to 131×10^{-3} SI (basalt sample), spanning more than five orders of magnitude.

SM30 measurement was performed with the short axis of the sample along the coil axis, as would be expected for a rock resting naturally on the ground. The sample was placed directly on the SM30 probe in order to have a zero background susceptibility. The average of up and down measurements (i.e. on both sides of the pebble) is denoted by M. The average deviation between the two measurements is 10 per cent. A few samples show larger deviations (up to 40 per cent), linked to a section being far from elliptical (e.g. triangular). The ratio M/K_r, called the geometric factor α, represents the correction factor that has to be applied to SM30 measurements in order to obtain the real volume magnetic susceptibility ($K = M/\alpha$). After discarding eight outliers corresponding to samples with volume susceptibility lower than 50×10^{-6} SI, the trend as a function of sample volume is practically the same for the four sets of samples (Fig. 2). This confirms that the geometric factor does not depend on the magnetic susceptibility. For the limestone a marginally significant higher α appears, due to a flatter mean shape (see below) and smoother surface. This empirical calibration curve can be parametrized, and the equations obtained along different segments of the curve allow the evaluation of the volume magnetic susceptibility of a natural sample of known volume with a single SM30 measurement performed at contact with the sample. For large samples, α is around 0.74. In order to estimate more precisely the geometric factor for infinite objects, we performed a set of SM30 measurements on a $40 \times 20 \times 20$ cm homogeneous clay body with flat sides and obtained $K = (172 \pm 3) \times 10^{-6}$ SI. Compared with $K = (195 \pm 2) \times 10^{-6}$ SI obtained with the KLY2, we have $\alpha_0 = 0.88$. It should be noted that to achieve absolute calibration of the SM30, an additional multiplication factor of 1.06 should be introduced in order to take into account the absolute calibration of the KLY2 (Sagnotti *et al.* 2003). However, in this paper we report uncorrected KLY2 values.

Table 1. Physical characteristics of pebbles used for calibration.

Type	n	ρ (10^3 kg m^{-3})	K (10^{-6} SI)			F			V (cm^3)		
			Mean	Min.	Max.	Mean	Min.	Max.	Mean	Min.	Max.
I	56	2.62	140	−1	525	0.43	0.20	0.64	26.84	1.21	130
II	60	2.63	7320	220	26297	0.47	0.20	0.85	28.78	0.59	145
III	144	2.9	41212	126	79369	0.57	0.27	0.86	18.14	0.29	145
IV	112	2.79	47262	1015	131408	0.58	0.37	0.89	49.75	0.42	271
V	15	2.07	195	195	195	0.61	0.40	0.94	516	45.7	1000

Key: I, marly limestone; II, phonolite and agpaite; III, basalts; IV, porphyric basalts; V, clay; n, number of samples; ρ, mean density; K, volume susceptibility; F, flattening parameter (see text); V, volume.

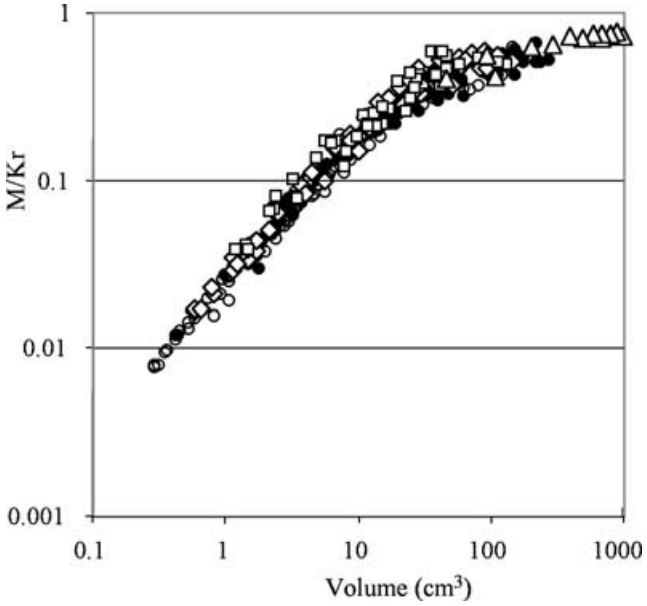

Figure 2. Geometric factor versus sample volume for the four sets of pebbles (empty boxes, marly limestones; diamonds, phonolites and agpaites; empty circles, basalts; full circles, porphyric basalts; triangles, clay). Note log scales. For marly limestones, only samples with volume susceptibility above 50×10^{-6} SI are plotted. Note the log scale for volume.

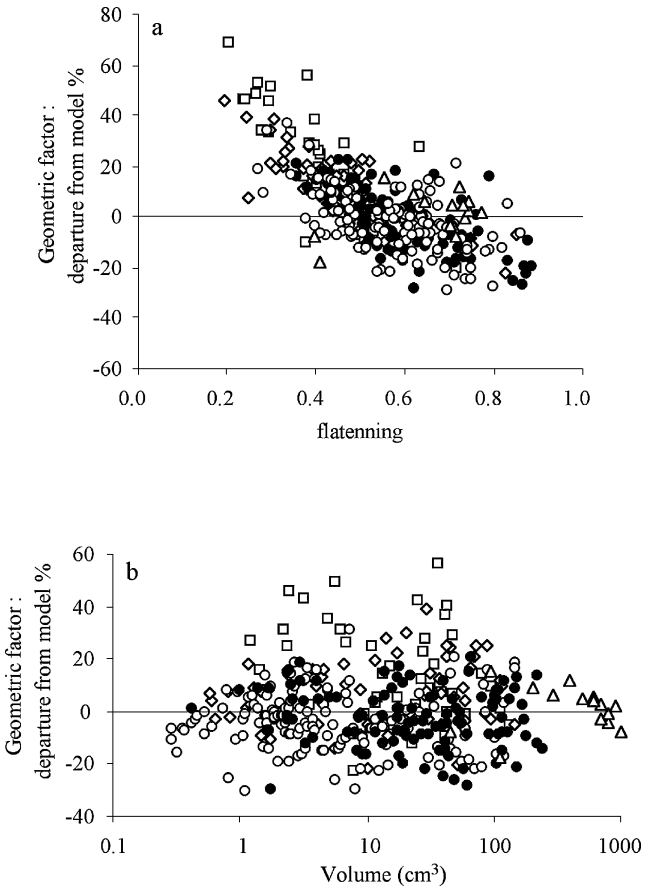

Figure 3. (a) Relative difference between the geometric factor computed from our model and the measured value versus flattening of the sample. (b) Relative difference between the geometric factor computed from our model and the measured value versus volume of the sample. Symbols as on Fig. 2. Note the log scale for volume.

For a given volume, the relative variability of α around the mean is about 10 per cent. This variability is due to the variable shape of the pebble as demonstrated by Fig. 3 that shows the evolution of the relative α scatter versus the flattening of the sample defined as $F = c/\sqrt{ab}$ where a, b and c are the long, intermediate and short axis of the ellipsoid used to describe the sample. It appears that the parametrization of the curve is closest to reality for objects with F around 0.5 (Fig. 3a). For flatter or more rounded objects, a correction up to $\pm$20 per cent (for most common natural shapes) should be applied. For some unusually flat shapes, the correction can reach 50 per cent. On the other hand, the differences between the model and the measurements do not depend on the volume of the sample (Fig. 3b). A possible refinement would be to take into account the shape of the measured sample for a more precise evaluation of magnetic susceptibility from a single SM30 measurement.

Another approach of SM30 calibration can be found in Jordanova *et al.* (2003).

4 VALIDATION

We are currently developing a magnetic classification scheme for meteorites. Rochette *et al.* (2003) showed that for a given group of ordinary chondrites, magnetic susceptibility was restricted to a narrow range and that this property allows the distinction between the three groups LL, L and H. Besides being a fast and powerful control tool for meteorite classification, this result demonstrates that *in situ* measurements on extraterrestrial bodies such as planets, asteroids or comets can bring crucial information about for instance the meteorite class they can be attributed to (Rochette *et al.* 2004). When the NEAR probe landed on 433 Eros asteroid in 2001 February, magnetic susceptibility measurements at the surface could have given clues to whether 433 Eros could be the parent body of a given group of ordinary chondrites. This question was not solved by the chemical and mineralogical probes available onboard NEAR.

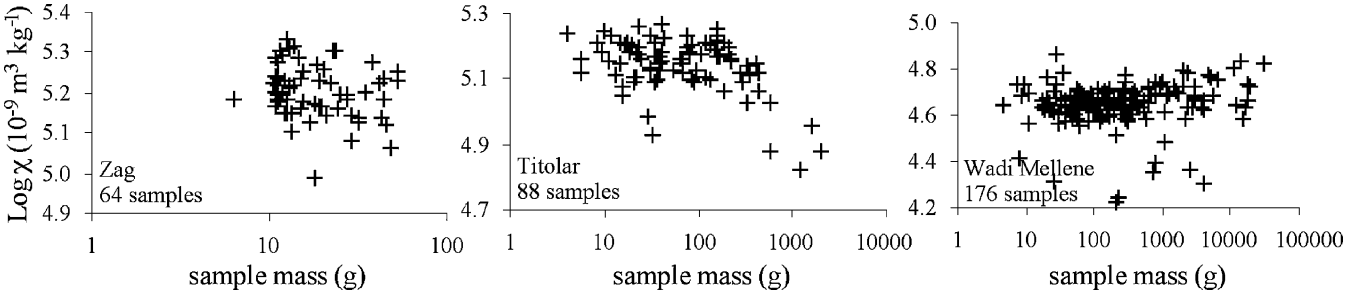

Figure 4. Magnetic susceptibility (in 10^{-9} m^3 kg^{-1} for comparison with Rochette *et al.* 2003) versus sample mass for the three studied meteorite falls (boxes, Wadi Mellene; circles, Zag; diamonds, Titolar). Note the log scale for volume.

In order to check the validity of the SM30 calibration, we performed measurements on a number of ordinary chondrite samples from Zag (H3-6), Wadi Mellene (L3.8, A. Jambon personal communication, 2003) and Titolar (not yet classified). The samples, from three different suspected meteorite falls (i.e. collected within the same area of a few square kilometres) were found in the Sahara desert by M. Franco. For such uncut raw samples, the magnetic susceptibility was determined using the SM30 measurements and the calibration curve defined in the previous section. Sample volume was determined by dividing its mass by its average density (taken from Consolmagno & Britt 1998). To compare with Rochette *et al.* (2003) we used the decimal log of the specific susceptibility χ (in 10^{-9} m^3 kg^{-1}). The good coherence of the data (Fig. 4) indicates that the calibration law for the SM30 is essentially correct for use with natural objects. In particular there is no relation between the volume and the volume susceptibility of the samples that would indicate a bias in the calibration. Only a few values appear to be significantly lower than the mean value: they are either the results of measurements performed on surfaces with complex non-planar geometry or real outliers, either from anomalously highly weathered pieces or from unpaired meteorites. In particular the four Titolar samples of large mass responsible for an apparent negative correlation of $\log \chi$ with mass could be of another type. When compared with the Rochette *et al.* (2003) database, these measurements confirm that chondrites Zag ($\log \chi = 5.23$, s.d. $= 0.07$) and Wadi Mellene ($\log \chi = 4.68$, s.d. $= 0.10$) belong to the H and L groups respectively, and strongly suggest that Titolar ($\log \chi = 5.16$, s.d. $= 0.08$), that has not been classified yet, belongs to the H group. The obtained s.d. compare well with the average s.d. of 0.1 given by multiple fragments of the same meteorite measured with the KLY2 (Rochette *et al.* 2003).

5 2-D MODELLING OF SM30 MEASUREMENTS

5.1 Modelling

The second step of calibration is to consider non-homogeneous samples, and in particular horizontal layering of magnetic susceptibility as can be found in soils or in the case of a rock sample lying on a soil. The response of the SM30 over its integration volume was evaluated by performing measurement of an infinite homogeneous body with increasing distance. This homogeneous body was a concrete cylinder (40 cm in diameter, 20 cm high) described in Lecoanet *et al.* (1999). The SM30 was mounted on a retort stand equipped with a millimetre scale. The measurements with increasing distance are displayed on Fig. 5. It appears that the penetration depth of this instrument is about 6 cm and that 90 per cent of the signal come from the first 2.5 cm. It could be easily increased by using a larger coil, the penetration depth being comparable to the diameter of the coil. The curve in Fig. 5 has been parametrized by a sixth-degree polynomial equation denoted $S(x) = M(x)/M(0)$ where $M(x)$ is the SM30 measurement at a distance x from the concrete block. If we call $R(x) = dS(x)/dx$, the SM30 measurement at a distance d from a horizontally layered body is

$$M(d) = \alpha_0 \int_{x=+\infty}^{x=d} R(x)K(x)\,dx \tag{1}$$

where $K(x)$ is the volume magnetic susceptibility of the layer of thickness dx at a distance x from the SM30 (Fig. 6). Eq. (1) allows the modelling of the SM30 response when measuring samples that have infinite (i.e. >8 cm) horizontal dimensions and susceptibility varying along x only. Note also that $1/\alpha_0\,[1 - S(x)]$ is the correction

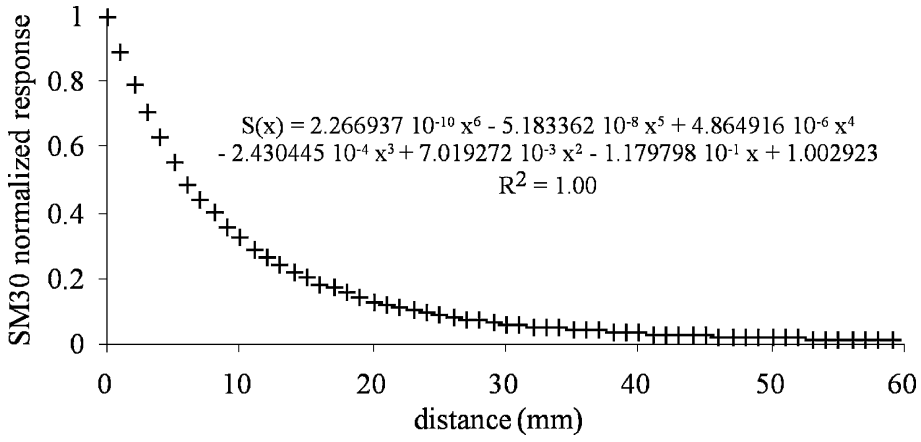

Figure 5. SM30 response versus measuring distance for a homogeneous concrete block representing an infinite sample.

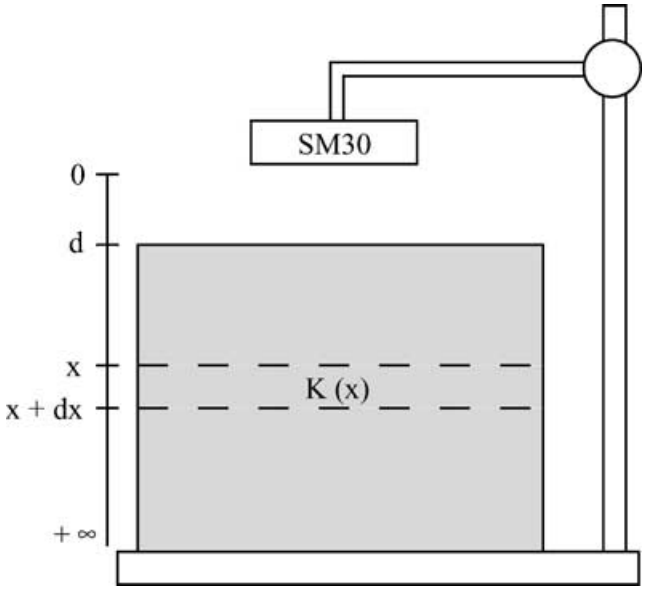

Figure 6. Experimental setting for measurement at different distances of vertically layered infinite samples.

factor to be applied to the SM30 measurement at contact of a slice of thickness x and horizontal dimensions >8 cm.

5.2 Experimental validation

In the case of a homogeneous infinite body of volume magnetic susceptibility K_0, eq. (1) gives $M(d) = \alpha_0 K_0 S(d)$. In the case of a two-layer body with susceptibility and thickness K_1 and t_1 (upper part), K_2 and t_2 (lower part), eq. (1) gives

$$M(d) = \alpha_0 K_2 \int_{x=t_2+t_1+d}^{x=t_1+d} R(x)\,dx + \alpha_0 K_1 \int_{x=t_1+d}^{x=d} R(x)\,dx$$

that can be written

$$M(d) = \alpha_0 K_2 [S(t_1 + d) - S(t_2 + t_1 + d)] + \alpha_0 K_1 [S(d) - S(t_1 + d)]. \quad (2)$$

We performed measurement on a synthetic two-layer body composed of an upper layer (tile) of susceptibility $K_1 = 7100 \times 10^{-6}$ SI and thickness $t_1 = 11.6$ mm and a lower layer (concrete cylinder described before) of susceptibility $K_2 = 250 \times 10^{-6}$ SI and infinite thickness. Both layers are homogeneous. Eq. (2) predicts $M(d) = \alpha_0 K_2 S(t_1 + d) + \alpha_0 K_1 [S(d) - S(t_1 + d)]$. As we know K_1, K_2, t_1 and $S(x)$, we can compute $M(d)$. The SM30 measurements with increasing distance and the computed values are displayed in Fig. 7. The fit is excellent and confirms the validity of the calibration. The largest relative errors occur for measurements at distances above 45 mm because of the weak magnetic signal measured. The comparison between the trend of SM30 measurements with increasing distance and $S(x)$ (representing the trend for a homogeneous infinite body) is a way to check for homogeneity of the measured sample. Large departures from $S(x)$ increasing with depth, as shown by the thick solid line in Fig. 7, indicate that the measured body is not homogeneous but horizontally layered. From this kind of curve it is indeed possible to infer if susceptibility decreases (studied case) or increases with depth. In the first (respectively second) case normalized measurements decrease faster (respectively slower) than $S(x)$ and $M(x)/S(x)$ is a decreasing (respectively increasing) function.

5.3 Inversion of measurements

We now show how it is possible to invert the SM30 measurements in order to estimate a vertical susceptibility profile. The synthetic sample used is the same that in the preceding section, i.e. a two-layer body with an infinite lower layer. We consider that the susceptibility of the lower layer, K_2, is known. This situation could correspond to the natural case where the lower layer is a soil whose susceptibility can be measured elsewhere, enclosing an outcropping rock of unknown thickness and susceptibility. Two SM30 measurements are performed at distances d_1 and d_2. From eq. (2), we have

$$M(d_1) = \alpha_0 K_2 S(t_1 + d_1) + \alpha_0 K_1 [S(d_1) - S(t_1 + d_1)]$$

and

$$M(d_2) = \alpha_0 K_2 S(t_1 + d_2) + \alpha_0 K_1 [S(d_2) - S(t_1 + d_2)]. \quad (3)$$

The only unknowns are K_1 and t_1, and the thickness t_1 is obtained by resolving

$$f(t_1) = K_2 S(t_1 + d_2) + \frac{M(d_1)/\alpha_0 - K_2 S(t_1 + d_1)[S(d_2 - S(t_1 + d_2)]}{S(d_1) - S(t_1 + d_1)} - M(d_2)/\alpha_0 = 0. \quad (4)$$

This was done for a set of two measurements ($d_1 = 10$ mm and $d_2 = 30$ mm) and gives $t_1 = 11.0$ mm. This result is in close agreement with the real value of 11.6 mm (Table 2), which confirms the

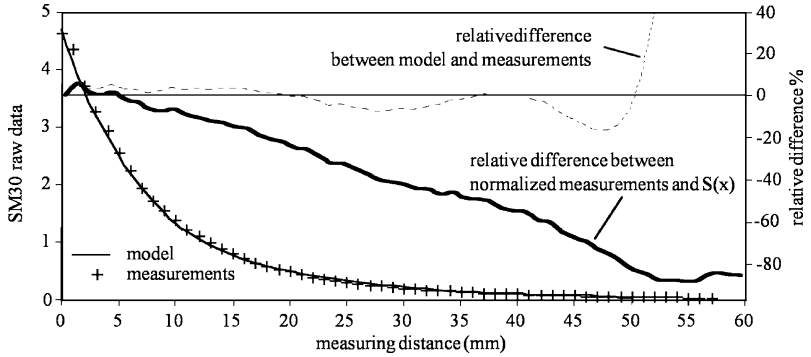

Figure 7. Comparison between experimental measurements (crosses) and computed values (solid line) for a two-layer composite sample. The dotted line indicates the relative difference between measurements and the model. The thick solid line is the relative difference between normalized measurements and $S(x)$.

Table 2. Computed and measured values for the inverse problem of a two-layer composite sample.

	t_1 (mm)	K_1 (10^{-6} SI)
Measured	11.6	7100
Computed	11.0	7440
Relative difference	5 per cent	5 per cent

Key: t_1, thickness of upper layer; K_1, volume susceptibility of upper layer.

validity of the modelling and inversion. The K_1 value derived from the computed t_1 value is also very close to the measured value. It must be noted that if both K_1 and K_2 had been unknown, a set of three SM30 measurements at different distances would have allowed the full determination of the structure of the composite body (K_1, K_2 and t_1).

6 DETERMINATION OF VOLUME BY A MAGNETIC METHOD

As the SM30 measures only the part of the sample that lies within the integration volume, it should be possible to assess the volume of a sample by comparing two measurements performed at different distances from the sample. For the 371 natural pebbles used for calibration of discrete sample measurements, we performed, in addition to the initial measurement at contact (denoted M_0), two measurements at a distance of 8 mm (denoted M_1) and 16 mm (denoted M_2). For these three measurements, the sample was placed directly on the SM30 probe in order to have a zero background susceptibility. The ratios M_0/M_1 and M_1/M_2 actually depend on the volume of the measured samples (Fig. 8) and it appears that the ratio M_0/M_1 (respectively M_1/M_2) allows the estimation of the sample volume in the range 0.2 to 20 cm^3 (respectively 20 to 200 cm^3). For the M_0/M_1 graph the outliers correspond to samples with volume susceptibility lower than 400×10^{-6} SI, whereas for the M_1/M_2 graph even samples with a susceptibility around 10×10^{-6} SI follow the general trend. This is an innovative non-destructive method for estimating the volume of a sample smaller than 200 cm^3, with no need to manipulate, touch or even see the sample. However, it can only be applied to homogeneous samples, and for samples smaller than 20 cm^3 it can be applied only when the susceptibility is above 400×10^{-6} SI. Fig. 9 shows that the volume computed from the parametrization of the curves of Fig. 8 is generally in the range ±40 per cent of the real volume, the precision being better for smaller objects.

With this possibility of determining the volume of a sample, we can propose a measurement scheme to evaluate the volume magnetic susceptibility of a discrete sample with the SM30 only. Three measurements have to be performed: at contact (M_0), at 8 mm (M_1) and at 16 mm (M_2). The ratios M_0/M_1 and M_1/M_2 allow the determination of sample volume. This volume is then used to infer the geometric factor α of the sample (Fig. 2). Finally, the volume susceptibility is equal to M_0/α. This scheme could be easily automated and could be validated for instance during a robotized meteorite collection campaigns in Antarctic blue ice fields. Successful field demonstrations have already been undertaken by the Nomad robot of the Robotics Institute at Carnegie Mellon University, Pittsburgh, USA (Apostopoulos *et al.* 2000). With an SM30-like sensor mounted on a mobile arm, the volume magnetic susceptibility of a discrete sample, even partly hidden in the ice or covered with snow, would be rapidly determined with enough precision to distinguish between meteorites and terrestrial rocks, greatly increasing the meteorite recognition rate of such a robot. Moreover, Antarctic blue ice

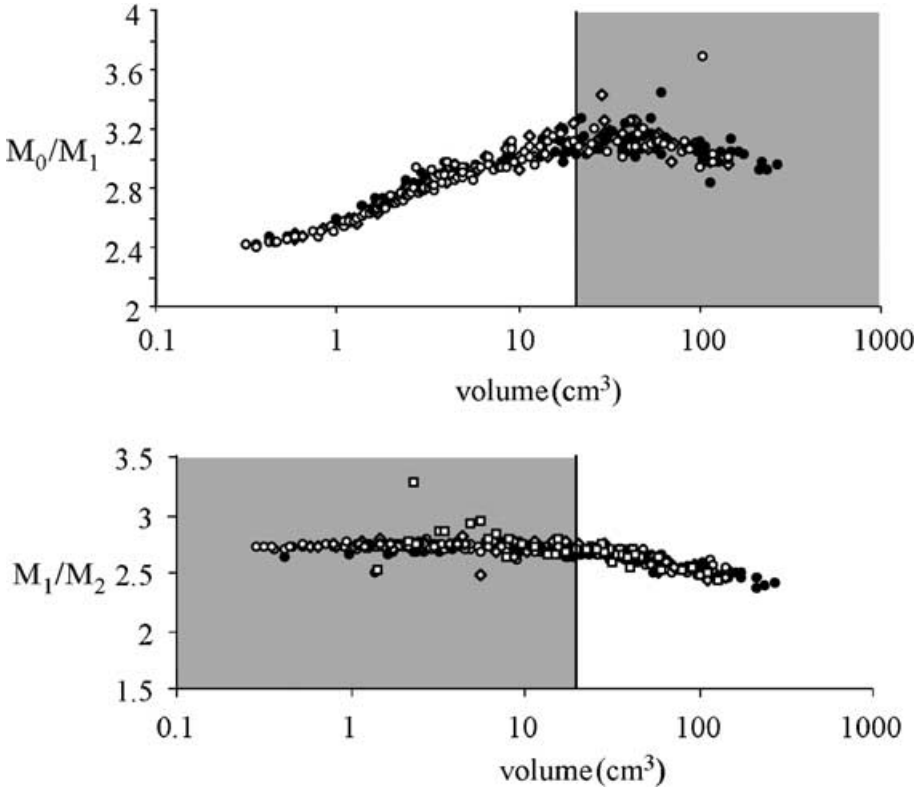

Figure 8. M_0/M_1 versus volume (top) and M_1/M_2 versus volume (bottom). For the top graph, samples with volume susceptibility below 400×10^{-6} SI are not plotted. Symbols as on Fig. 2.

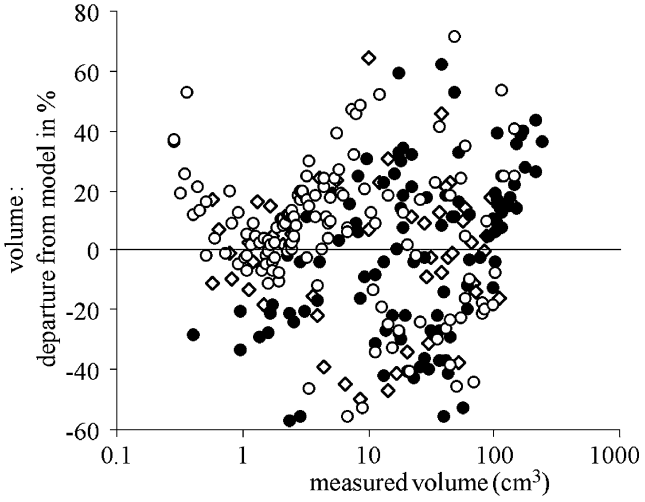

Figure 9. Relative difference between the volumes computed from our model and the measured volumes in per cent. Symbols as on Fig. 2.

is the ideal location for using *in situ* automated susceptibility measurements as the samples rest directly on the ice that has a negligible magnetic susceptibility of -9×10^{-6} SI. On a planetary surface, samples would rest on a substratum with a magnetic susceptibility possibly close to that of the samples. In this case, the magnetic susceptibility of the substratum would have to be measured separately in order to compute the background contribution and isolate the sample's magnetic signature.

We tested the proposed measurement scheme (including volume determination by the magnetic method) on 18 ordinary chondrite fragments (on loan from the Museum National d'Histoire Naturelle (MNHN), Paris, France and some private collections). All these fragments but three (Park, Waconda and Wadi Mellene) are from meteorite falls. Most of them have been sawed and present sharp edges and angular unnatural shapes. The results are then compared with the value given by the KLY2 measurements associated with the volume determined using sample mean density (taken from Consolmagno & Britt 1998) and mass (Table 3, Fig. 10). The mean difference between the two values is 43 per cent. This rather large error is attributable in part to the strong anisotropy of the magnetic susceptibility of the measured samples (ranging from 1.06 to 1.54 with a mean value of 1.32) and in part to the lack of precision in estimating the volume of very irregular objects by the magnetic method. Indeed the mean difference between the volume determined by our magnetic method and the volume determined by weight and density is 38 per cent. If we use the latter volume for both susceptibility measurements, the mean difference between KLY2 and SM30 measurements is reduced to 16 per cent (Fig. 10b), which indicates that the SM30 calibration is also valid for very angular objects.

Despite the observed departures, it must be noted that the precision obtained with the magnetic measurement scheme (Fig. 10a) is sufficient to distinguish ordinary chondrites from almost all types of terrestrial rocks and to classify most of the ordinary chondrites into the three groups LL, L and H. After verification, the 'Ness County' sample appeared to be a mislabelled and unidentified sample in the MNHN collection. As shown in Fig. 10(a), only two samples (Tathlith and the unusually strongly magnetic Gifu sample) are misclassified (H instead of L) by the SM30 measurement scheme. Our previously reported measurements on natural rounded stones (Fig. 2) suggest that the success rate may be higher with less angular natural samples.

7 CONCLUSION

The SM30 calibration performed on pebbles of variable shape, size and lithology allows the measurement of volume magnetic

Table 3. Magnetic susceptibility of 18 ordinary chondrite samples.

Meteorite	Group	K_{KLY2} (10^{-6} SI)	K_{SM30} (10^{-6} SI)	Diff.$_1$ (per cent)	K'_{SM30} (10^{-6} SI)	Diff.$_2$ (per cent)	V_d (cm^3)	V_m (cm^3)	Diff.$_3$ (per cent)	P_{ams}
Alfianello	L	25 5641	409 896	60	256 610	0	0.54	0.31	43	1.49
Colby (Wisconsin)	L	287 435	180 188	37	232 015	19	8.45	12.11	43	1.47
Fisher	L	272 046	197 636	27	293 250	8	6.88	11.30	64	1.42
Gao-Guenie 2*	H	499 475	396 747	21	–	–	2.38	–	–	–
Gifu	L	402 081	491 060	22	276 375	31	4.51	2.28	49	1.54
Hallingeberg	L	195 970	389 121	99	189 765	3	3.39	1.46	57	1.11
Hollbrook	L	125 883	91 339	27	137 464	9	7.91	14.46	83	1.25
Kilabo*	LL	11 829	9828	11	10 500	9	6.40	5.14	20	1.09
Krymka	LL	45 972	37 828	18	33 155	28	5.64	4.72	16	1.40
Leedy	L	261 236	175 929	33	160 447	39	5.23	4.58	12	1.36
'Ness County'	L	674 317	417 374	38	536 444	20	10.10	16.00	58	1.44
Olivenza	LL	20 739	27 776	34	19 379	7	3.14	2.03	35	1.15
Oued El Hadjar*	LL	42 702	37 484	12	48 131	13	1.87	2.44	30	1.16
Park	L	99 376	240 981	142	123 879	25	4.38	2.00	54	1.07
Tathlith	L	271 487	573 848	111	240 551	11	1.73	0.63	64	1.38
Tennasilm	L	218 870	276 220	26	222 153	2	2.98	2.27	24	1.07
Waconda	L	274 526	295 605	8	180 842	34	10.52	5.82	45	1.39
Wadi Mellene*	L	181 348	157 978	13	–	–	92.73	–	–	–

Key: K_{KLY2}, volume susceptibility measured with KLY2 and volume estimated by weight and density; K_{SM30}, volume susceptibility measured with SM30 and volume estimated by magnetic method; K'_{SM30}, volume susceptibility measured with SM30 and volume estimated by weight and density; V_d, volume estimated by weight and density; V_m, volume estimated by the magnetic method; P_{ams}, degree of anisotropy of magnetic susceptibility; Diff.$_1$, relative difference between K_{KLY2} and K_{SM30}; Diff.$_2$, relative difference between K_{KLY2} and K'_{SM30}; Diff.$_3$, relative difference between V_d and V_m; *, samples from private collections. 'Ness County' is a mislabelled sample.

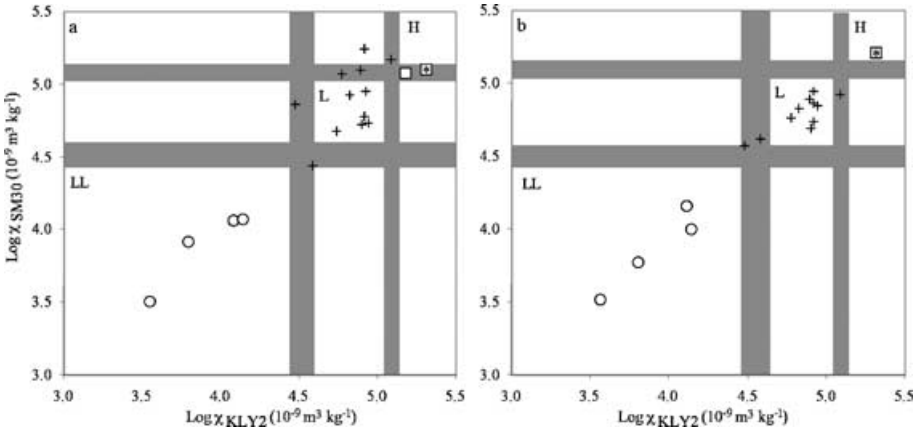

Figure 10. (a) Volume susceptibility determined by SM30 (including volume determination) versus volume magnetic susceptibility determined with KLY2 for H (boxes), L (crosses) and LL (circles) ordinary chondrite samples. (b) Volume susceptibility determined by SM30 (with volume determined by weight and density) versus volume magnetic susceptibility determined with KLY2. Shaded areas delimitate the LL, L and H susceptibility range (from Rochette *et al.* 2003). For comparison, terrestrial rocks would all plot below 4.0. The star indicates the mislabelled Ness County sample.

susceptibility of discrete samples of natural shape. The calibration performed on a semi-infinite homogeneous body with variable measuring distance leads to a 2-D model of the SM30 response over its integration volume and allows one to check for sample homogeneity and to determine susceptibility profiles with a sufficient number of discrete measurements at variable distance. Both types of calibration have been successfully validated on natural or synthetic samples. The calibration on discrete pebbles also shows that the volume of a sample can be evaluated with two to three measurements at different distances. This new method of determining volume is then integrated in a measurement scheme that provides the volume magnetic susceptibility of a discrete boulder with two to three measurements.

Therefore the SM30 portable susceptometer appears to be a suitable instrument with which to perform *in situ* magnetic susceptibility measurements on individual boulders or to establish magnetic susceptibility profiles that are of interest in soil sciences or weathering studies for example. It represents a precise penetrative iron phase probe, and its low electric consumption, weight and small dimensions (180 g and 10 × 6 × 2 cm including case, sensors and electronics) add to the relative simplicity of the proposed measurement scheme should enable the SM30 to be used for automatic *in situ* susceptibility measurements. Such automated measurements would be of interest for robotic exploration of any solid body of the solar system, or automatic meteorite collection mission in Antarctic blue ice fields.

ACKNOWLEDGMENTS

We are indebted to M. Franco who welcomed one of us (PE) to measure his collection, as well as to M. Denise from MNHN Paris, for the loan of other meteorite samples. Z. Hulka is thanked for providing various characteristics of the SM30 and for upgrading it to measure up to 1 SI. The manuscript benefited from constructive reviews by two anonymous reviewers. This contribution was supported by the Planétologie programme of INSU-CNRS and CNES.

REFERENCES

Apostopoulos, D.S., Wagner, M.D., Shamah, B.N., Pedersen, L., Shillcutt, K. & Whittaker, W.L., 2000. Technology and field demonstration of robotic search for Antarctic meteorites, *Int. J. Robotics Res.,* **19,** 1015–1032.

Consolmagno, G.J. & Britt, D.T., 1998. The density and porosity of meteorites from the Vatican collection, *Met. Planet. Sci.,* **33,** 1231–1241.

Heller, F., Strzyszcz, Z. & Magiera, T., 1998. Magnetic record of industrial pollution in forest soils of Upper Silesia, Poland, *J. geophys. Res.,* **13,** 17 767–17 774.

Ishihara, S., 1977. The magnetite series and ilmenite series granitic rocks, *Mining Geol.,* **27,** 293–305.

Jordanova, D., Veneva, L. & Hoffmann, V., 2003. Magnetic susceptibility screening of anthropogenic impact on the Danube river sediments in northwestern Bulgaria – Preliminary results, *Stud. Geophys. Geod.,* **47,** 403–418.

Lecoanet, H., Leveque, F. & Segura, S., 1999. Magnetic susceptibility in environmental application: comparison of field probes, *Phys. Earth planet. Inter.,* **115,** 191–204.

Mathé, P.E., Rochette, P., Vandamme, D. & Colin, F., 1999. Volumetric changes in weathered profiles: iso-element mass balance method questioned by magnetic fabric, *Earth planet. Sci. Lett.,* **167,** 255–267.

Rochette, P., Gattacceca, J., Menvielle, M., Eisenlohr, P. & Chevrier, V., 2004. Interest and design of magnetic properties measurements on planetary and asteroidal landers, *Planet. Space Sci.,* in press.

Rochette, P., Sagnotti, L., Consolmagno, G., Denise, M., Folco, L., Gattacceca, J., Osete, M. & Pesonen, L., 2003. Magnetic classification of stony meteorites: 1. Ordinary chondrites, *Met. Planet. Sci.,* **38,** 251–268.

Sagnotti, L., Rochette, P., Jackson, M., Vadeboin, F., Dinarès-Turell, J., Winkler, A. & Mag-Net Science Team, 2003. Inter-laboratory calibration of low-field magnetic and anhysteretic susceptibility measurements, *Phys. Earth planet. Inter.,* **138,** 25–38.

Thouveny, N. *et al.,* 1994. Climate variations in Europe over the past 140 kyr deduced from rock magnetism, *Nature,* **371,** 503–506.

Touchard, Y. & Rochette, P., 2004. Determining tephra fall deposit thickness in sedimentary record from magnetic susceptibility curve: example of four Ethiopian tephras, *Geochem. Geophys. Geosyst.,* **5,** Q01009, doi:10.1029/2003GC000628.